

# STUDY OF ELECTROLYTE FLOW AT ELECTROCHEMICAL FINISHING

Ionuț Alexandru Bunea<sup>1,2</sup>, Albert Georgian Păun<sup>1</sup>, Liviu-Daniel Ghiculescu<sup>1</sup>, Cornel-Cristian Enciu<sup>1</sup>

<sup>1</sup>POLITEHNICA University of Bucharest, <sup>2</sup>Center for Advanced Laser Technologies, National Institute for Laser, Plasma and Radiation Physics (INFLPR), [alexandru.bunea@inflpr.ro](mailto:alexandru.bunea@inflpr.ro), [albert\\_georgian02@yahoo.es](mailto:albert_georgian02@yahoo.es), [daniel.ghiculescu@upb.ro](mailto:daniel.ghiculescu@upb.ro), [cornel.enciu@upb.ro](mailto:cornel.enciu@upb.ro)

**ABSTRACT:** The paper presents the current state of the electrochemical polishing process (Electro Chemical Machining – ECM), using the intermittent flow method of the electrolytic liquid. The uniformity of the flow rate on the machined surface was aimed for, a key condition for ECM polishing. The logical scheme of the study and numerical simulations of the flow were developed for three different machining surfaces, in the following cases: laminar flow, turbulent flow and flow stop. The distributions of flow velocities in the machining gap were determined. The results of the simulations were validated by experimental data that determined an optimal value for the current density on the machined surface at which a maximum decrease in roughness was achieved.

**KEYWORDS:** electrochemical, electrolyte flow, surface roughness, numerical simulation.

## 1. INTRODUCTION

Electrochemical machining (ECM) has multiple advantages, one of them being a very high machining rate because it is based on simultaneous anodic dissolution of the entire machined surface [1,2]. Moreover, it is a concentrated energy technology with another advantage of any hardness, without inducing tool wear and internal stress in the surface layer, but limited to electrically conductive materials. In ECM, the high velocity and pressure of the electrolyte in the work gap (the space between the tool and the part) is important to remove gas bubbles, heat, dissolved (precipitated) material from the part and to maintain the stability of the ECM (electrochemical reactions) [9, 10]. In case of uneven flow of the electrolytic liquid on the processed surface, striations appear. Therefore, keeping the electrolyte flow under control is very important in the ECM process [4]. ECM has a wide range of applications in fields such as: electronic, automotive, aerospace, medical, food, nuclear, etc. through the ability of ECM to create mirror-like surfaces [1, 5].

The work aims to develop an intermittent processing method, which includes several phases [11, 12]: the first phase involves a high flow rate of the electrolyte [13, 14], for washing the machining working gap, and the second phase, a reduced flow rate during the current pulses, to allow a controlled polishing of the surface and to discourage the formation of the passivated layer [2].

## 2. SETUP

Schematically, an ECM process contains a tool - cathode and a workpiece - anode, with the electrolyte introduced under pressure through the gap between

them. The electrolyte outlet section (adjustable by valve) allows flow control. The fluid flow in the working gap is usually turbulent, which prevents the uniformity of the machining process [1, 2, 3, 5].

Patent EP 0 471 086 A1 (figure 1) presents an innovative device and process for the electrochemical polishing of metal surfaces, through a uniform distribution of electric current and the introduction of electrolytic liquid intermittently with varying flow rates. The patented technical solutions ensure a laminar type of flow during the electrical impulses to process the part uniformly, as well as a turbulent type of flow between them to ensure the adequate washing of the working gap [3].

In figure 2, the logic diagram of the numerical simulation is presented, while in figure 3, the equipment with which the operation will be performed is presented.

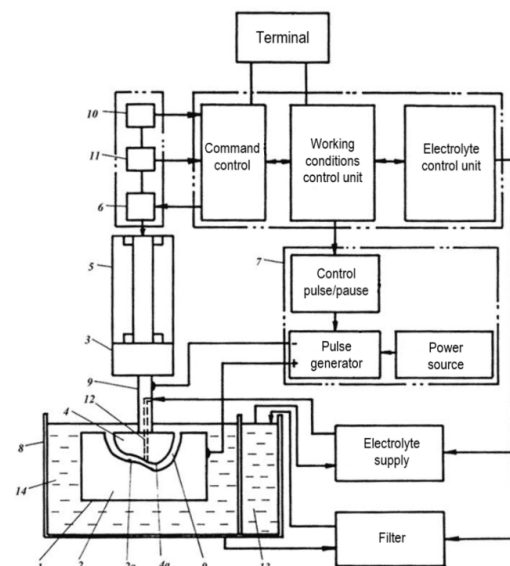


Figure 1. Intermittent ECM machining device [2,3]

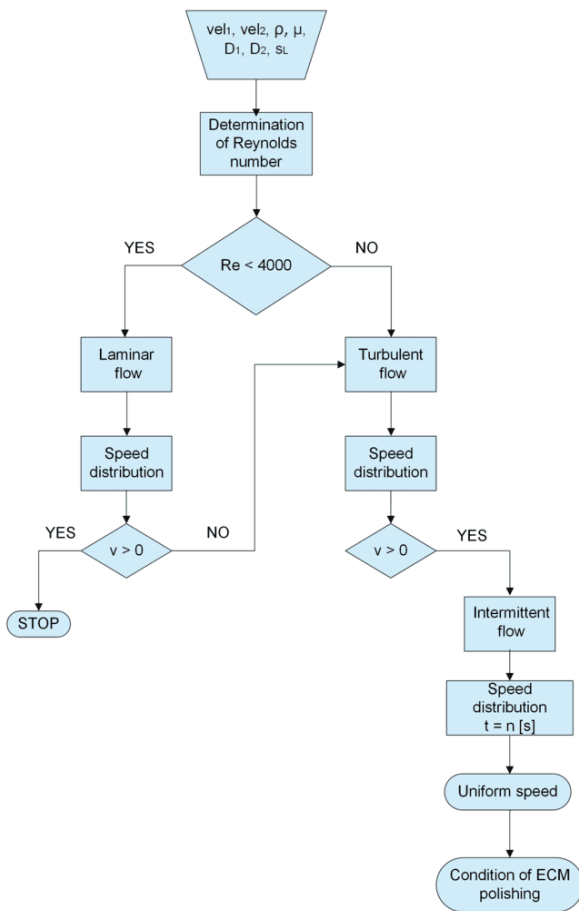


Figure 2. Logical diagram of the numerical simulation process

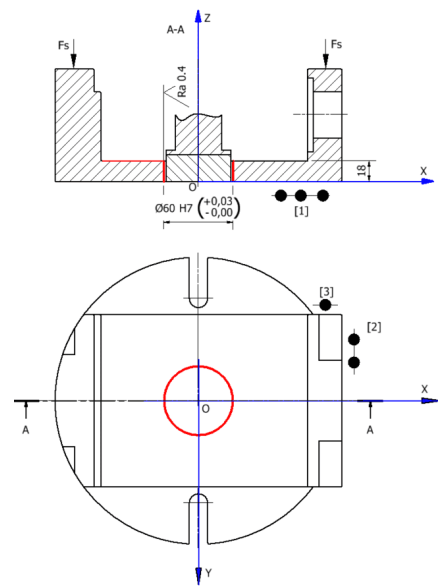


Figure 4. The machined surface for workpiece 1

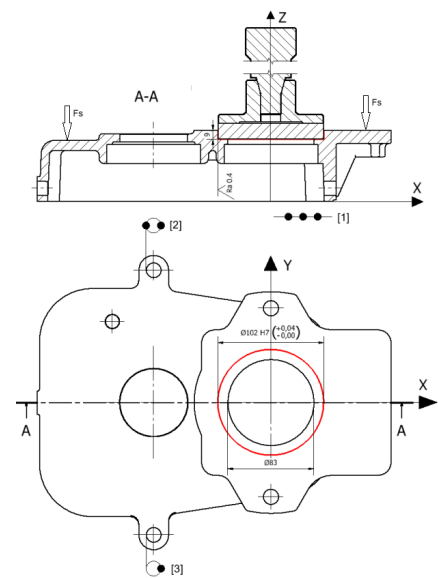


Figure 5. The machined surface for workpiece 2

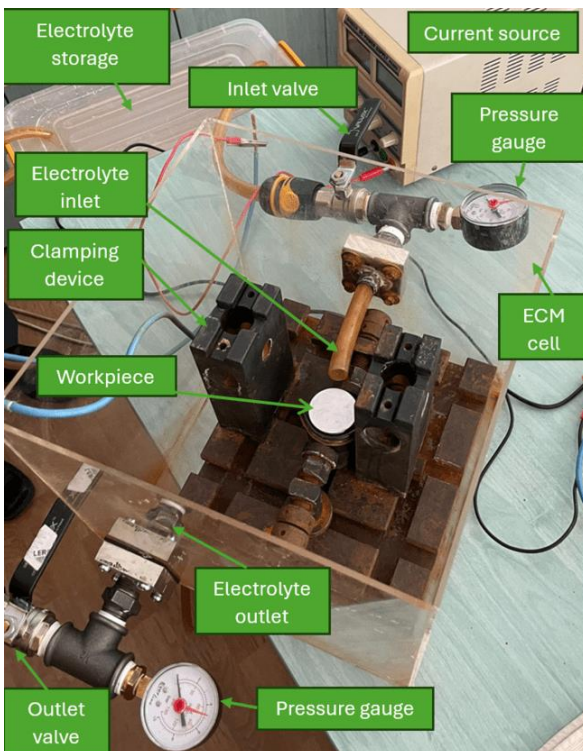


Figure 3. The equipment for electrochemical polishing made by As. Dr. Ing. C. Enciu

### 3. DETERMINATING REYNOLDS NUMBER

Reynolds number is calculated, which determines the type of flow (laminar or turbulent) using relation (1). For  $Re < 4000$ , the flow is laminar, respectively turbulent for  $Re \geq 4000$  [1]:

The wavelength ( $\lambda$ ) is calculated using formula 1:

$$Re = \frac{\rho \cdot vel \cdot l}{\mu} \quad (1)$$

where:  $\rho$  – fluid density [ $kg/m^3$ ];  $vel_1, vel_2$  – electrolyte inlet flow speed [ $m/s$ ];  $l$  – characteristic length [ $m$ ];  $\mu$  – dynamic viscosity of the liquid [ $Pa \cdot s$ ].

Two values of the flow velocity are introduced and used in the numerical simulation, from relation (1),  $vel_1 = 1.5 m/s$ , respectively  $vel_2 = 0.02 m/s$ :

$$Re_1 = \frac{\rho \cdot vel_1 \cdot l}{\mu} = \frac{1031 \cdot 1.5 \cdot 0.054}{0.00079} = 111583 > 4000 \rightarrow \text{turbulent flow}$$

The third figure shows the equipment used for experiments, made by As. Dr. Eng. C. Enciu, and figures 4, 5, 6 show the polished ECM surfaces for which the numerical simulations were carried out.

$$Re_2 = \frac{\rho \cdot vel_2 \cdot l}{\mu} = \frac{1031 \cdot 0,02 \cdot 0,054}{0,00079} = 1049,5 < 4000 \rightarrow \text{laminar flow}$$

#### 4. NUMERICAL SIMULATION OF THE ELECTROLYTE FLOW THROUGH THE MACHINING GAP

The steps required for modeling using COMSOL Multiphysics 4.2 are described:

**Step 1.** The 3D module is chosen as the workspace, then Fluid Flow, Laminar Flow, and as Time dependent regime, in case 1, for vel1. [2, 8].

**Step 2.** Parameterization of the model and introduction of the characteristics of the electrolyte liquid is done according to table 1 respectively table 8. 5% NaCl electrolyte properties are introduced:

**Table 1.** Modeling parameters from Global definitions

Name	Expression	Value	Description
rp	30 [mm]	0.03 [m]	Workpiece radius
hp	18 [mm]	0.018 [m]	Machining gap height
vel1	0.02 [m/s]	0.02 [m/s]	Flow speed 1
tc1	5 [s]	5 [s]	Time under flow speed 1
vel2	1,5 [m/s]	1,5 [m/s]	Flow speed 2
tc2	5 [s]	5 [s]	Time under flow speed 2
tc3	1 [s]	1 [s]	Time under closed inlet valve
xl	0,69 [mm]	6.9 E-4 [m]	Machining gap
Pout	2000000 [Pa]	2000000 [Pa]	Pressure of liquid at the exit
hi	30 [mm]	0.03 [mm]	Hole height at the entry point

**Table 2.** Introduction of electrolyte properties ( 5% NaCl)

Property	Name	Value	Unit	Property group
Density	Rho	1031	Kg/m <sup>3</sup>	Basic
Dynamic viscosity	mu	0.79/1000	Pa*s	Basic

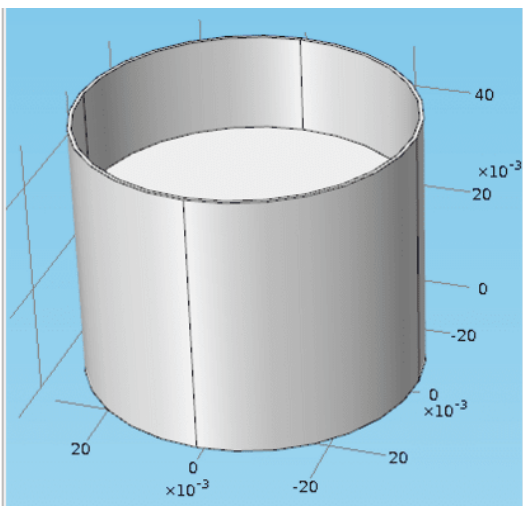


**Figure 6.** Creation of the geometry of the machining gap

**Step 3.** Creating the flow geometry parameterized by the prior step sizes (figure 7) and discretizing it by fine-sized free tetrahedral finite elements in the geometry node of the Model Builder (figure 8).

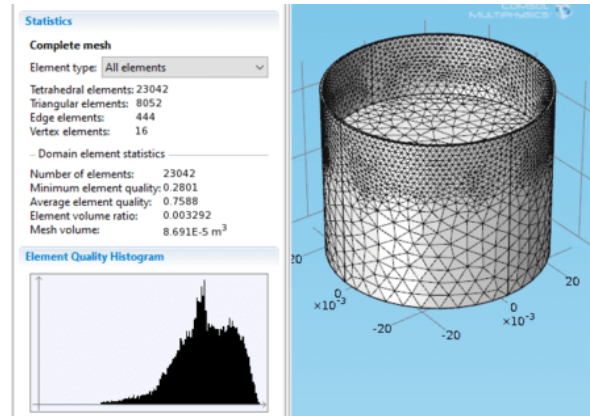


**Figure 7.** Discretization of geometry in finite elements

**Step 4.** Setting boundary conditions, presented in in figure 9, in the form of a velocity (vel1/vel2) input and the output under pressure (pout) of the liquid (figure 10) in the case of laminar flow:

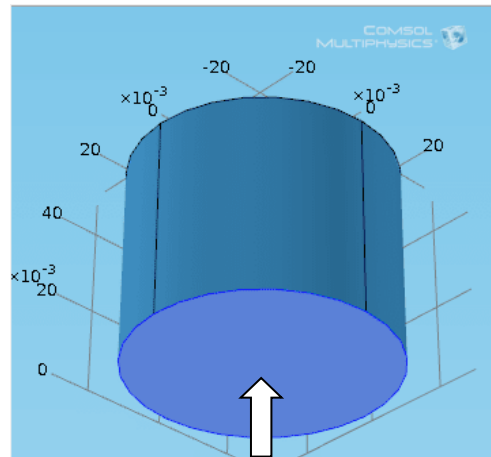


**Figure 8.** Selecting the inlet

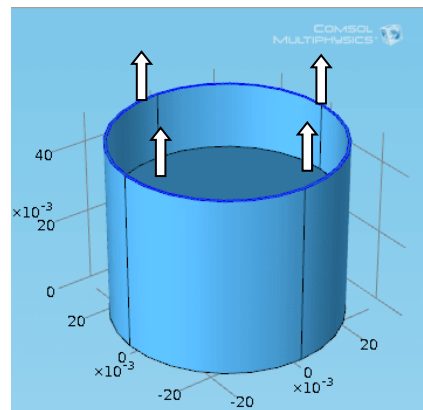


**Figure 9.** Selecting the outlet

**Step 5.** Flow simulation is done from the Study module, for each flow. Time parameters can be chosen in the case of the time dependent study for laminar flow (Study 1) (figure 11). The second study is set for turbulent flow (Study 2) (figure 12).

We also set the flow for the case of cancellation of the inlet flow velocity, whose input data are the results of the previous simulation (Study 2), the turbulent flow (figure 13).

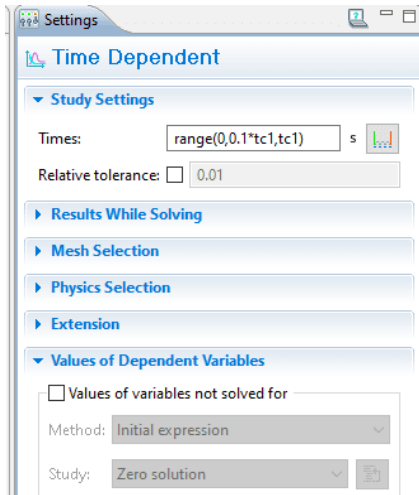


**Figure 10.** Setting of laminar flow  
**Figure 11.**

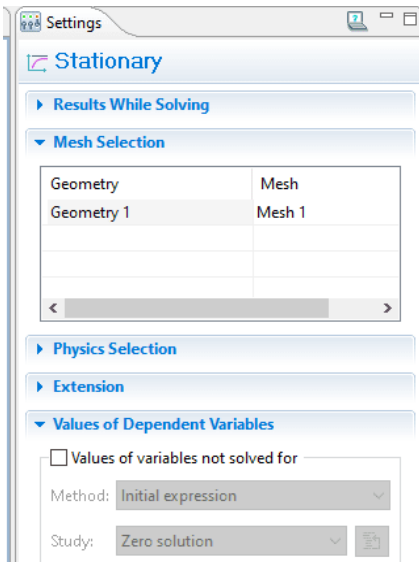


**Figure 12.** Setting of turbulent flow

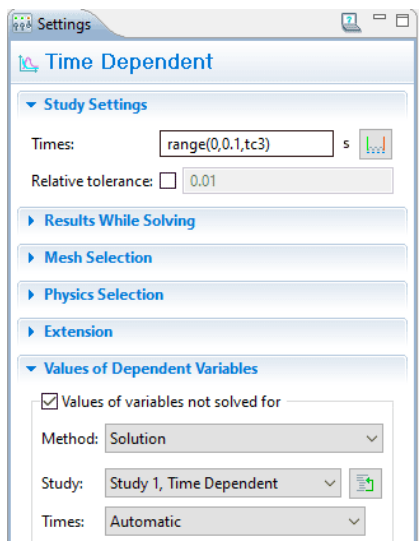


**Figure 13.** Setting of laminar flow stop

## 5. INTERPRETATION OF THE RESULTS

In laminar flow, it is found that the velocity is cancelled in certain areas of the machining gap [2], [6, 7], (figure 14.). In figure 15, the pressure reduction on the flow path from the processing gap is highlighted. Therefore, the turbulent flow solution is adopted, by increasing the inlet velocity, at vel1. It can be seen from figure 17 that the flow velocity does not cancel, which allows washing of the machining gap, but the velocity distribution is not uniform over the machined surface. Finally, the flow velocity at the electrolyte inlet is cancelled and the flow velocity distribution is obtained after a time of 5 s, figure 18. Even if the velocity is not constant, its values are so small that the electrolytic liquid is considered stationary. At this point, one can proceed to the ECM polishing phase (the flow uniformity condition being met). Figures 16 and 19 show the distribution of velocities along the electrolyte path. The sequence shown is repeated for model 2, shown in figures 20-25.

Below are the results for workpiece number 1:

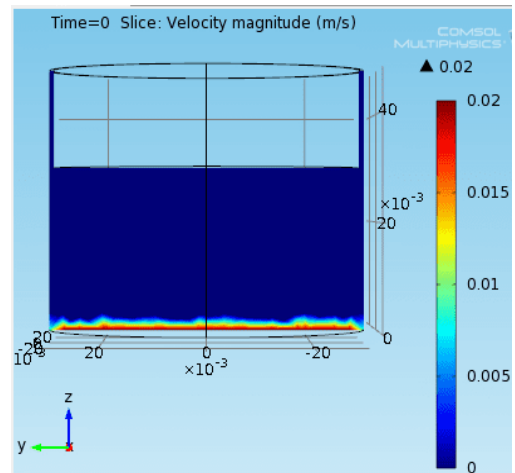


**Figure 14.** Electrolyte velocity distribution in the machining gap, in laminar flow

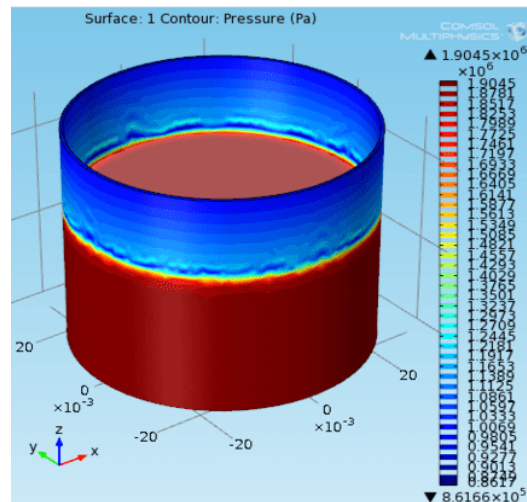


**Figure 15.** Fluid pressure during turbulent flow

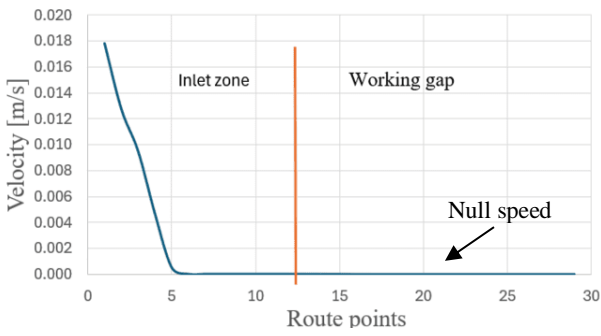


**Figure 16.** Velocity distribution along the electrolyte path for laminar flow ( $vel_1 = 0.02 \text{ m/s}$ )

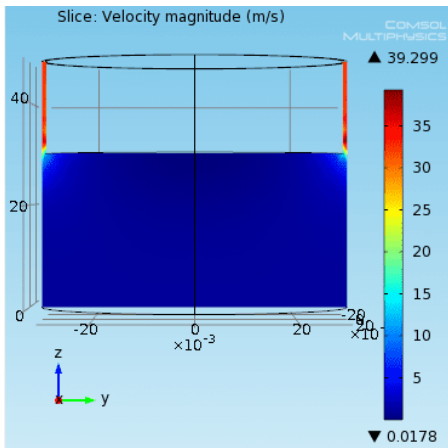


**Figure 17.** Electrolyte velocity distribution in the machining gap, turbulent flow

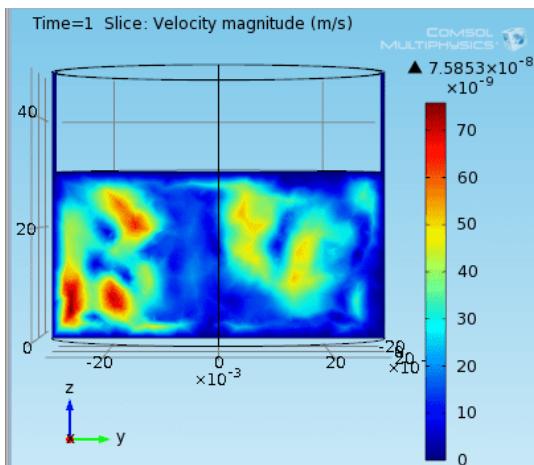


**Figure 18.** Velocity distribution in the machining gap after cancelling the input velocity, at  $t=5 \text{ s}$

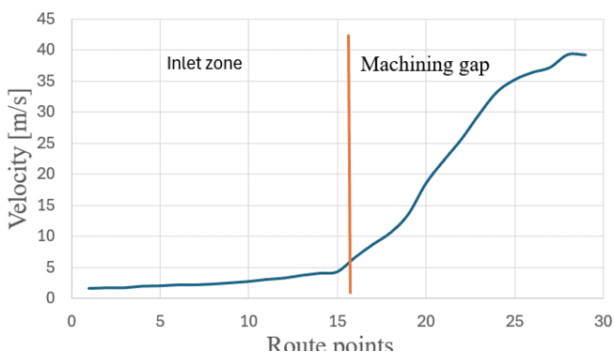


**Figure 19.** Velocity distribution along the electrolyte path for turbulent flow ( $vel_2 = 1.5 \text{ m/s}$ )

The results for workpiece number 2:

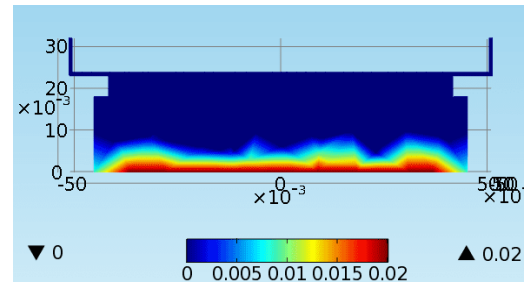


**Figure 20.** Electrolyte velocity distribution in the machining gap, in laminar flow

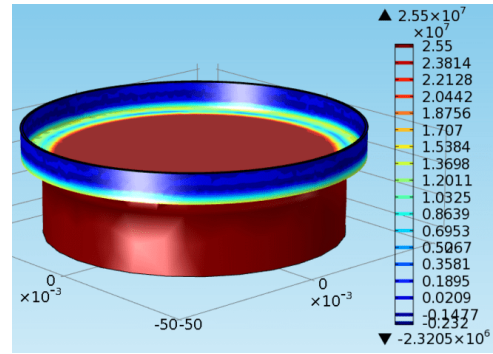


**Figure 21.** Fluid pressure during turbulent flow

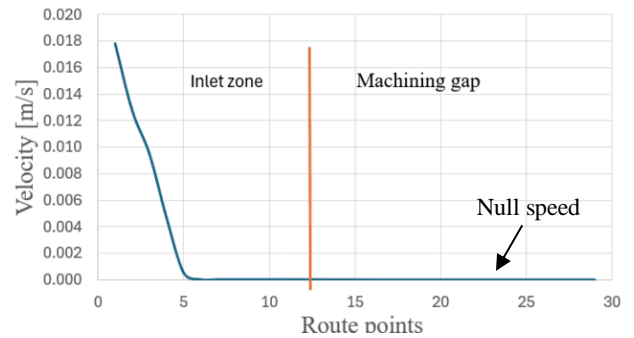


**Figure 22.** Velocity distribution along the electrolyte path for laminar flow ( $vel_1 = 0.02 \text{ m/s}$ )

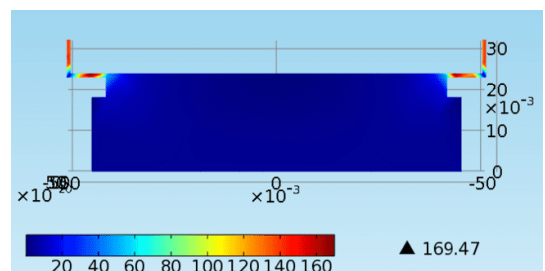


**Figure 23.** Electrolyte velocity distribution in the machining gap, turbulent flow

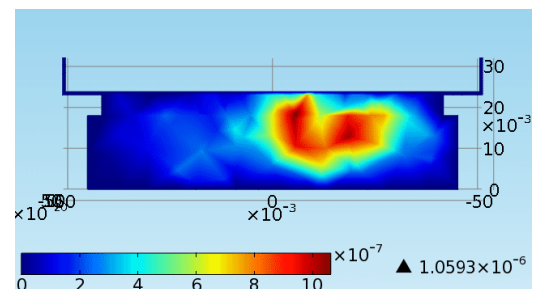


**Figure 24.** Velocity distribution in the machining gap after cancelling the input velocity, at  $t=5 \text{ s}$

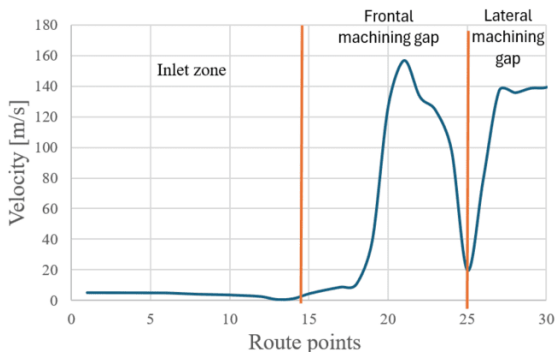


**Figure 25.** Velocity distribution along the electrolyte path for turbulent flow ( $vel_2 = 2$  m/s)

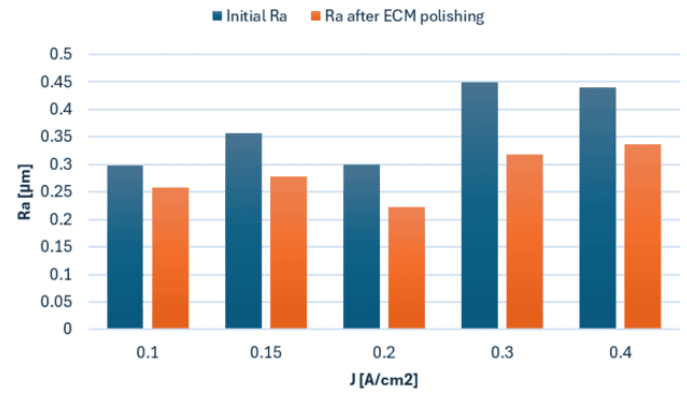


**Figure 27.** Variation of Ra as a function of current density J

Below are the results for workpiece number 3:

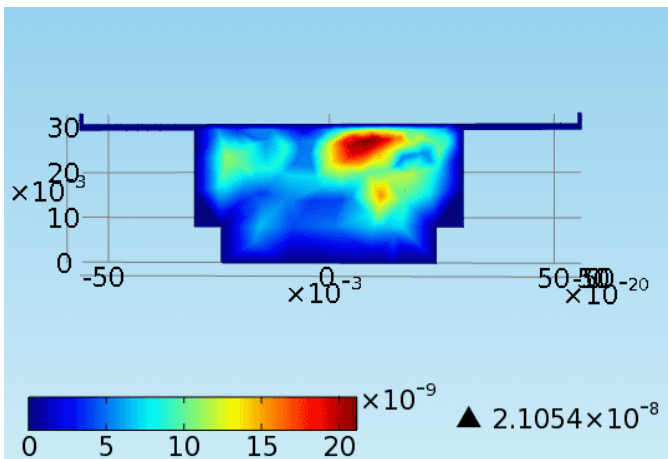


**Figure 26.** Electrolyte velocity distribution in the machining gap, in laminar flow

## 6. EXPERIMENTAL RESULTS

The experimental results obtained by the method of intermittent electrolyte flow and ECM finishing, 3 min, an area of  $4.9 \text{ cm}^2$  of a stainless steel with 12% Cr, (see figure 3) are presented in table 3:

**Table 3.** Resulted roughness in relation with the current density

J [A/cm²]	I [A]	Initial Ra [µm]	Final Ra [µm]	Ra roughness [%]
0,1	0.5	0.298	0.258	13.4
0,15	0.75	0.356	0.278	21.9
0,2	1	0.3	0.223	25.7
0,3	1.5	0.449	0.318	29.2
0,4	2	0.44	0.373	15.2

The graphical representation of the roughness as a function of the current density (J) on the machined surface (figure 32) shows that the maximum decrease of Ra is obtained at  $J=0.3 \text{ A/cm}^2$ .

An SEM QUANTA INSPECT F50 image of the machined surface (figure 33) shows uneven sampling of the material due to light-colored Cr carbide particles less than  $1 \text{ µm}$  in size, usual in the composition of stainless steel with 12% Cr.

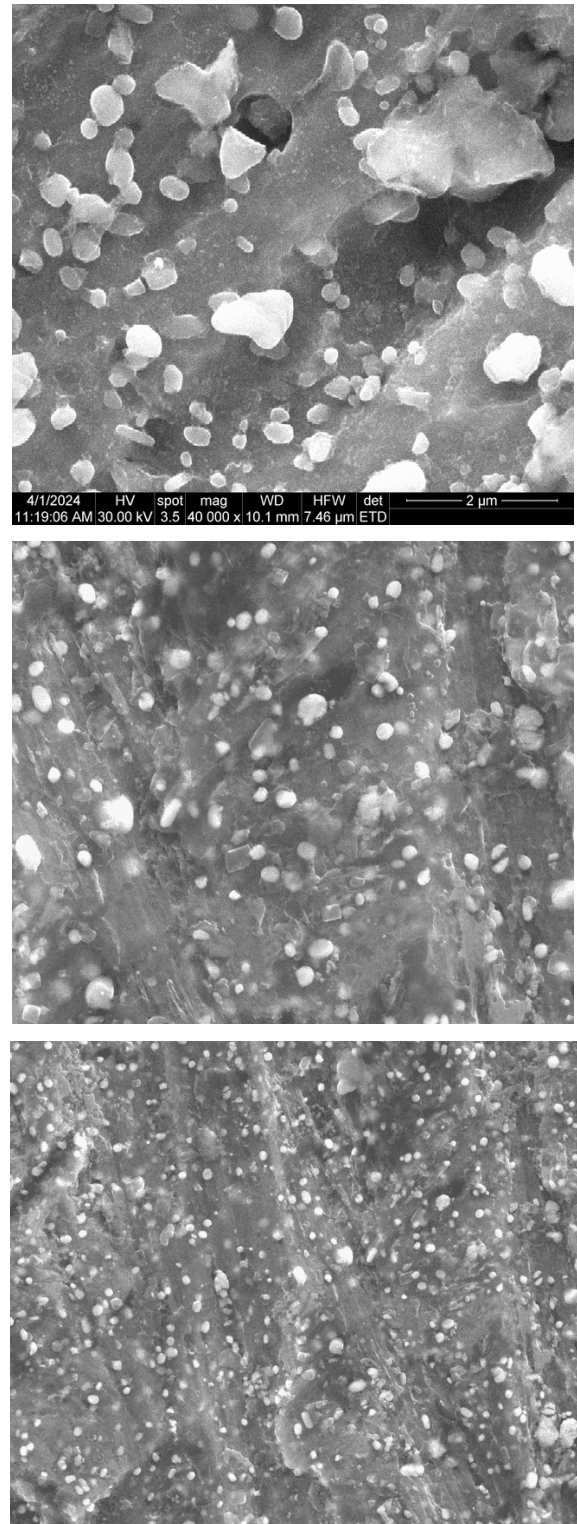


**Figure 28.** SEM images of the machined surface

## 7. CONCLUSIONS

The contributions of the work are the numerical simulation of the electrolyte flow during the polishing (finishing) of the ECM, according to a logical scheme that aimed to smooth the flow on the processed surface.

This was achieved by applying the following phases:

- Laminar flow simulation to check the speed distribution in the processing area.
- Turbulent high-speed flow for washing the machining working gap, respectively removing the resulting ECM products.
- Stopping the flow after 5s and proceeding with ECM for 3 minutes.

The experimental results obtained, which validated the numerical simulations, highlight the decrease of about 25% of Ra by this method of ECM over a stainless steel with 12% Cr.

SEM images show non-uniform material sampling due to Cr-carbide particles in the stainless-steel composition.

## 8. FURTHER RESEARCH

Potential areas for further research include:

- a. Optimizing the current density on the processed surface.
- b. The use of a more efficient electrolyte for stainless steel processing.
- c. Optimizing its concentration and temperature.
- d. Optimizing the processing gap.
- e. Improvement of the experimental stand (electrolyte filtration, temperature, and PH control in real time).

## 9. REFERENCES

1. Ghiculescu, D., Contributions to Development and Innovation of Ultrasonically Aided Nonconventional Machining, Teză de abilitare, UPB 2016.
2. Marinescu, N.I., Ghiculescu, D., Popa, L., Pîrnău, C., Marinescu, R., Ene, G.M., Procese tehnologice cu fascicule, oscilații și jeturi, Volumul 3, Tehnologii cu unde ultrasonice, ISBN 978-606-23-0984-8, Editura Printech, Cod CNC SIS 54, București, 2019.
3. Kuwabara Y, Hukuroi-shi S., *Electrolytic finishing method*, EP 0 471 086 A1.
4. Hongping L, Dahai M., *Characteristics of ECM polishing influenced by workpiece corner feature and electrolyte flow*, in: M. Kunieda, R.K. Leach:

*Precision Engineering*, vol. 56, Elsevier, pag. 330-342, ISSN: 1873-2372, (2019).

5. Chagnes, A., Chapter 2 - Fundamentals in Electrochemistry and Hydrometallurgy, in: A. Chagnes, J. Światowska: *Lithium Process Chemistry*, pag. 41-80, Elsevier, ISBN: 978-0-12-801417-2, (2015).
6. L.G., Leal, *Laminar Flow and Convective Transport Processes*, 143030, Elsevier, ISBN: 978-0-7506-9117-8, (1992).
7. R.K., Shah, A.L., London, *Laminar Flow Forced Convection in Ducts*, Elsevier, ISBN: 978-0-12-020051-1, (1978).
8. T., Cebeci, *Analysis of Turbulent Flows with Computer Programs*, Elsevier, ISBN: 978-0-08-098335-6, (2013).
9. Hassan, E.H., *Vibration-assisted electrochemical machining: a review*, The International Journal of Advanced Manufacturing Technology, Vol. 105, p. 579-593, (2019).
10. Saxena, K.K., Qian, J., Reynaerts, D., *A review on process capabilities of electrochemical micromachining and its hybrid variants*, International Journal of Machine Tools and Manufacture, Vol. 127, p. 28-56, (2018).
11. Nicoara, D., Hedes, A., Sora, I., *Ultrasonic Enhancement of an Electrochemical Machining Process*, Proceedings of the 5th WSEAS International Conference on Applications of Electrical Engineering, Prague, Czech Republic, Vol. 5, p. 213-218, (2006).
12. Zhang, Y., *Investigation Into Current Efficiency For Pulse Electrochemical Machining Of Nickel Alloy*, Industrial and Management Systems Engineering, M.S. Thesis, University of Nebraska - Lincoln, (2010).
13. Katiyar, P.K., Randhawa, N. S., Hait, J., Jana, R.K., Singh, K.K., Mankhand, T.R., *Anodic Dissolution Behaviour of Tungsten Carbide Scraps in Ammoniacal Media*, In Advanced Materials Research, Vol. 828, p. 11-20, Trans Tech Publications, Ltd., (2013).
14. Reza, R.H., Mohammadreza, S., *Machining of 304 stainless steel Using Electrochemical Machining (ECM) Process: Response Surface Methodology Approach*, International Journal of Industrial Engineering & Production Research, Vol. 31, p. 397-407, (2020).